



## SYNTHESIS OF SiO<sub>2</sub>&GO-INCORPORATED TiO<sub>2</sub> NANOFIBERS AS EFFECTIVE PHOTOCATALYSTS FOR ORGANIC POLLUTANTS DEGRADATION

Gehan M.k. Tolba

Chemical Engineering Department, Faculty of Engineering, Minia university, Minia, Egypt

\*Corresponding author(s) E-mail: [jehan.kotb@mu.edu.eg](mailto:jehan.kotb@mu.edu.eg)

### Abstract

Azo dyes, such as reactive black 5 (RB5), are extensively employed in the textile industry due to their stabilities and simple dyeing procedures. About 50% of the amount of RB5 used is lost and discharged into nearby aquatic systems, causing chronic and acute toxicity. Therefore, it is necessary to treat the contaminated effluents before releasing them into the surroundings. The study synthesized SiO<sub>2</sub>&GO-doped titanium dioxide nanofibers with highly photocatalytic activity, utilizing the electrospinning method followed by calcination. Additionally, the study used SEM, FESEM, EDX, XRD, TEM analysis, and UV-vis data to characterize the morphology and the structures of the synthesized nanofibers. The photocatalytic activities of the produced nanofibers were examined for the removal of the reactive black 5 and reactive orange 16. The results showed that SiO<sub>2</sub>&GO-doped titanium dioxide nanofibers could eliminate 86 % of the reactive black within 2 h compared to 19 % removal of the reactive black 5 when using the pristine TiO<sub>2</sub> nanofibers. Moreover, the photocatalysts could be reused many times without any obvious changes in their stability and activity, suggesting a potential application for wastewater treatment.

**Keywords:** Titanium dioxide; Electrospinning; Photocatalytic; Nanofibers; Graphene oxide.

### 1. Introduction

Enormous studies have investigated TiO<sub>2</sub>'s powerful semiconductor capabilities in water splitting and environmental remediation [1]. In practice, the photocatalysis of the conventional TiO<sub>2</sub> has some barriers to treating the organic pollutants due to the low efficiency of absorption in sunlight. Many factors powerfully linked to synthesis and processing routes significantly influence the TiO<sub>2</sub> photocatalytic activity. These factors include morphology shape, particle size, particle aggregation, surface area, surface defects, surface hydroxyl group content, phase composition, and crystal structure[2, 3]. Moreover, researchers have proposed to increase the separation rate of the photoinduced carriers and extend the absorption threshold of TiO<sub>2</sub> to overcome those barriers. Therefore, different studies have examined several methods, such as doping of metal, coupling of semiconductors, deposition of noble metal, and non-metal modification [4, 5].

Doping can induce changes to the crystal and electronic structures of the parent metal, which gives rise to changes in the bandgap. Among the metals oxides used to improve the TiO<sub>2</sub> activities are graphene oxide and silica nanoparticles[6]. The remarkable properties of graphene oxide are thermal stability, the enhanced ability for electron-carrying, and large

surface area. Additionally, compared to its bulky structure, nano silica has distinguished properties, including surface chemical properties, low toxicity, a large ratio of its surface area to volume, and significant physical, thermal and chemical stability, bringing nano silica to many applications, such as colors and dyes removal with high recyclability in wastewater treatment [7, 8]. Therefore, many studies have combined or functionalized nano silica with different functional groups and molecules[9].

Dye houses, textile, paper, and printing industries extensively utilize synthetic dyes. Azo dyes are commercially the most produced dyes annually and the most characterized by at least one nitrogen-nitrogen double bond (-N=N-) and the bright color of their aqueous solutions. Reactive Black 5 (RB5) is one of the azo dyes widely used in the textile industry due to its stabilities and simple dyeing procedures. However, about 50% of the total amount of RB5 used is lost[10, 11]. Additionally, textile facilities dispose the untreated effluent in the surrounding environment, causing chronic and acute toxicity. Therefore, treating the dye bath effluents before releasing them into the nearby aquatic systems is necessary. Numerous technologies, such as adsorption, membrane process, electro-coagulation, and photocatalysis, were utilized in dye removal from wastewater[12].

One of the promising strategies to remove toxic organic contaminants from water is the combination of adsorption technology and the photocatalysis process. In the adsorption process, the adsorbents adsorb the dyes from wastewater to its surface. After that, photocatalytic degradation removes the adsorbed dyes. Therefore, developing materials that have high adsorption ability and good photocatalytic activity is crucial in wastewater treatment. As a result, several studies widely examined different adsorbents, such as mesoporous silica, alumina, and activated carbon, to modify the catalytic activity of  $\text{TiO}_2$ . [13, 14]

In the present study, silicon dioxide and graphene oxide nanoparticles, incorporated with titanium dioxide nanofibers, were developed for a photocatalytic process. The combination of  $\text{TiO}_2$  and  $\text{SiO}_2$  & GO could generate a synergistic effect, potentially achieving a photocatalyst with the optimized advantages of the three oxide elements, leading to enhance the photodegradation activity due to the potential enhancements in the absorbability and transfer rate of the efficient charge rate.

## 2. Experimental

### 2.1 Materials

Materials, such as N, N-dimethylformamide (DMF, 99.5 assays), and Titanium (IV) isopropoxide (Ti (Iso), 98.0 assay), were brought from Junsei Co. Ltd., Japan, while Poly (vinyl acetate) (PVAc, MW = 500,000 g/mol) and Reactive Black 5 (RB 5) dye were obtained from Sigma-Aldrich, USA. Silica nanoparticles and graphene oxide NPs were lab synthesized. The  $\text{SiO}_2$  NPs were synthesized using the hydrothermal method [7], while GO NPs were produced utilizing Hammer's method [15]. Furthermore, the present study used distilled water as a solvent. Moreover, this study used all materials, such as chemicals and reagents, as purchased without further purification and of analytical grade.

### 2.2 Nanofibers of $\text{SiO}_2$ and GO incorporated $\text{TiO}_2$ preparation

To prepare the nanofibers of  $\text{SiO}_2$  & GO incorporated  $\text{TiO}_2$ , the current study utilized electrospinning technology. First, titanium iso-propoxide (Ti (Iso)) and poly-vinyl acetate (PVAc, 14% by weight in DMF) were mixed at a ratio of 2:3 by weight, respectively, to prepare the sol-gel, followed by the addition of a few drops of acetic acid to the solution till it became clear. The solution is mixed at a temperature of 25 °C, utilizing a magnetic stirrer at a rotation rate of 150 rpm. The preparation of sol-gels containing  $\text{SiO}_2$  and GO involved the addition of 15% of GO and different amounts of the  $\text{SiO}_2$  dried powder (2% and 6% by

weight) to the solution to prepare the intended solutions, containing 2% and 6% by weight of  $\text{SiO}_2$  nanoparticles. After that, to homogeneously mix the solution, the obtained solution was vigorously stirred for 10 min at 25 °C. The source of the electric field used in the present study is CPS-60K02V1, Chungpa EMT Co., Republic of Korea, a high voltage power supply. The electrospinning of the prepared solution was carried out at 18 kV, a 15cm-working distance, 25 °C, and in a relative humidity atmosphere of 40%. The produced mats of nanofiber were primarily dried under vacuum for 24 h at a temperature of 80 °C. Then, they were calcined in the air at 680 °C for one hour with a 5 °C/min heating rate.

### 2.3 Characterization

The study utilized a scanning electron microscope; (JEOL Ltd., Japan) and a field-emission scanning electron microscope equipped with an EDX analysis tool (FESEM, Hitachi S-7400, Japan) to examine the surface morphology of nanofibers. Further, a Rigaku XRD (Japan), radiation over Bragg angle (10 to 80°), is used to study the crystallinity and phase while a transmission electron microscope (JEM-2010, Japan), operated at 200 kV, was employed to obtain high-resolution images. Furthermore, the study utilized a German HP 8453 UV-visible spectroscopy to investigate dye concentration during the photodegradation process. Moreover, the analysis of the obtained spectra obtained was performed using the HP ChemiStation 5890 Series software.

### 2.4 Measuring the Photocatalytic performance

The photocatalytic performance of the obtained catalyst was measured by degrading reactive black 5 dye solution. First, 20 mg of  $\text{TiO}_2/\text{GO}/\text{SiO}_2$  NFs were added to a 50 mL solution of 10 ppm RB5. Then, the obtained solution was irradiated under magnetic stirring and the lamp. After that, the samples were withdrawn at the same time intervals for the three consecutive cycles. After the centrifugal separation process, the study analyzed the supernatants using UV-Vis spectrometry at 595nm to determine RB5 concentrations in the solutions. The study consecutively performed each experiment three times to investigate the catalyst reusability. After each round, the catalyst is filtrated and washed. Then, new solutions that have the same RB5 concentration were employed.

## 3. Results and discussion

### 3.1. Characterization of the Produced Nanofibers

Figure 1 illustrates SEM images of the obtained  $\text{SiO}_2$ &GO/ $\text{TiO}_2$  composite nanofibers before and after

calcination. Figures 1A and 1B are for the concentration of 2% SiO<sub>2</sub>, while figures 1C and 1D are for 6% SiO<sub>2</sub>. As shown, the produced nanofibers possessed a satisfying morphology, continuous, smooth, randomly oriented nanofibers without any observed beads. Further, the incorporation of silica and graphene oxide in the nanofibers of TiO<sub>2</sub> did not negatively influence the morphology of the nanofibers. Moreover, the SEM photos, after burning the synthesized photocatalyst nanofibers in the air at 680 °C and after removing the polymer, show that the nanofibers remained smooth without any beads or roughness. However, the removal of the polymer decreases the diameter of the nanofiber. Additionally, the images show that as the concentration of the silica addition increases, the nanofibers become break down.

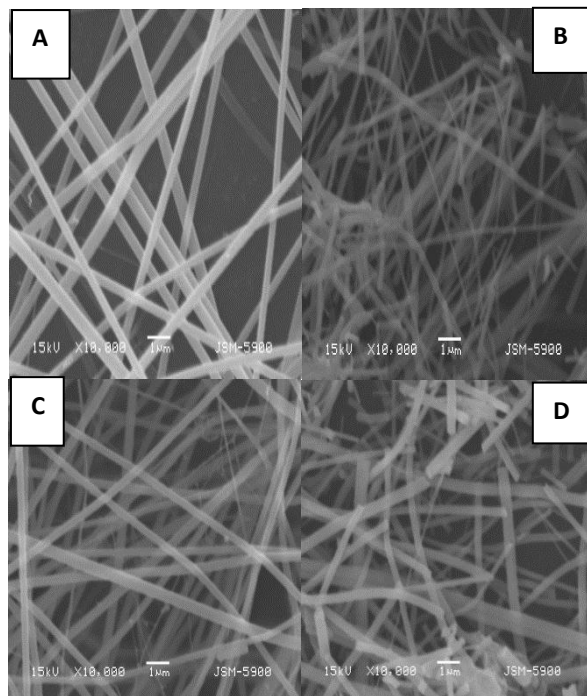


Figure 1: SEM images of the obtained SiO<sub>2</sub>&GO/TiO<sub>2</sub> photocatalyst; (A and B) for 2% SiO<sub>2</sub> before and after calcination, and (C and D) for 6% SiO<sub>2</sub> before and after calcination.

Figure 2 illustrates the FE-SEM images of the synthesized nanofibers after the prepared mats calcination for one hour at 680 °C. Although the calcination removed PVAc, the nanofibers were still continuous structures. Furthermore, FE-SEM EDX proves the existence of Si, O, Ti, and C. The EDX images demonstrate that the proposed calcination conditions produce pure silica, graphene oxide, and titanium dioxide.

The TEM image of the produced photocatalysts, as figure 3A illustrates, confirms the continuous nanofibrous structure synthesized after the calcination with good agreement with SEM & FESEM analysis. Further, the HRTEM image, as Figure 3B displays, shows better nanoparticles incorporated and homogeneously distributed in the titanium nanofibers. Moreover, The HRTEM image illustrates high crystallinity as parallel atomic planes for the crystalline TiO<sub>2</sub>, SiO<sub>2</sub>, and GO are detected. The samples show clear lattice fringes.

Moreover, the present study utilized XRD analysis to demonstrate the crystal phases of the calcined nanofibers. The synthesized NFs, as displayed in Figure 4, are composed mainly of the anatase phase, and the crystallinity of the anatase phase of TiO<sub>2</sub> is lower in the nanofibers containing SiO<sub>2</sub> and GO than the pure TiO<sub>2</sub> NFs, demonstrating the presence of the SiO<sub>2</sub> and GO NPs in the obtained nanofibers. The crystalline structure of TiO<sub>2</sub> is sensitive to any little additives to the electrospun solution since they form the rutile phase[16]. Furthermore, The observed peaks of the crystal planes of (101), (004), (112), (200), (105), (211), (204), (220), (220), and (215) at 2θ values of 25.091, 37.651, 38.441, 47.891, 53.891, 55.071, 62.401, 68.701, 70.041, and 75.001, respectively, demonstrate the formation of anatase TiO<sub>2</sub> [JCPDS card no. 21-1272], and free from any undesirable materials while the observed weak peaks indicate rutile TiO<sub>2</sub>. Moreover, as shown figure 4, no peaks were assigned to SiO<sub>2</sub> or GO. It might be due to the high dispersion of the nanoparticles through the TiO<sub>2</sub> lattice.

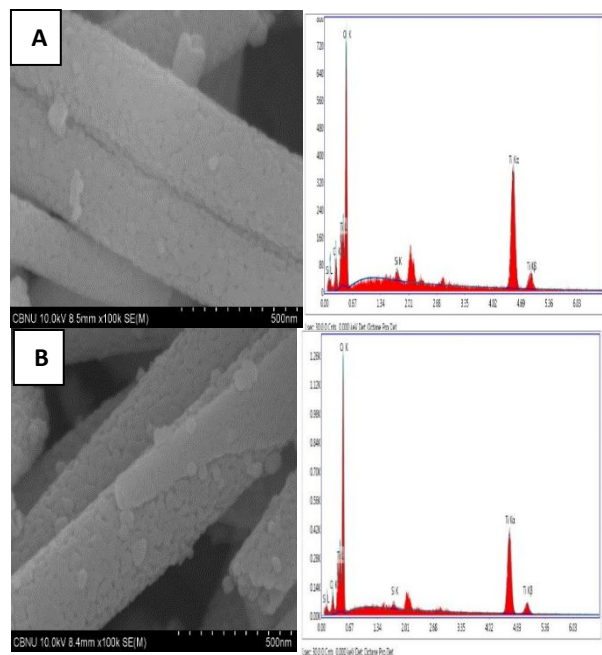


Figure 2: FESEM images of the obtained SiO<sub>2</sub>&GO/TiO<sub>2</sub> photocatalyst after calcination and EDX spectrometric data of SiO<sub>2</sub>&GO incorporated TiO<sub>2</sub> after calcination; A) 2% SiO<sub>2</sub>, B) 6%SiO<sub>2</sub>.

Figure 5 illustrates the UV–visible diffuse reflectance spectra of the TiO<sub>2</sub> nanofibers and the produced SiO<sub>2</sub>&GO/TiO<sub>2</sub>. As the figure displays, both SiO<sub>2</sub>&GO/TiO<sub>2</sub> catalyst and TiO<sub>2</sub> photo-absorbing curves have a similar shape. However, the presence of silica and graphene oxide nanoparticles with titanium dioxide exhibited a stronger absorption band than pure TiO<sub>2</sub> nanofibers. The absorption edge has a significant shift after the loading of SiO<sub>2</sub> and GO nanoparticles.

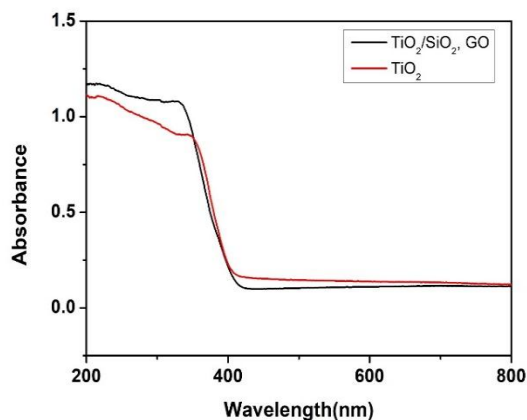


Figure 3: TEM image (A), and HRTEM (B) for the obtained SiO<sub>2</sub>&GO incorporated TiO<sub>2</sub>.

Based on the TiO<sub>2</sub> energy band structure, at a wavelength shorter than 400 nm, the optical absorption was primarily ascribed to the transmission of the electron from the valence to the conduction band. While at the visible-light region (ca. 400–550 nm), the weak optical absorption is primarily ascribed to the sub-band transitions, which are strongly linked to the oxygen vacancies of the TiO<sub>2</sub> surface, increased by the existence of GO and SiO<sub>2</sub> nanoparticles[17-19]. But the effect of interfacial coupling between GO and SiO<sub>2</sub>, and TiO<sub>2</sub> particles probably led to the black shift of the band gap. It might be due to a decrease in the band gap resulting from the addition of SiO<sub>2</sub> and GO [20].

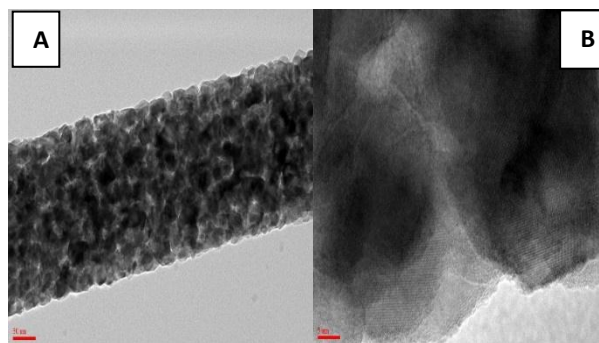


Figure 4: XRD pattern of the produced photocatalyst.

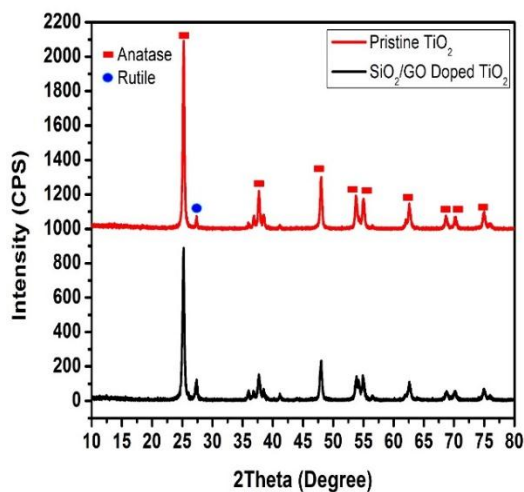


Figure 5: UV–visible diffuse reflectance spectra of TiO<sub>2</sub> and SiO<sub>2</sub>&GO/TiO<sub>2</sub>.

### 3.2. Performance of photodegradation

The photocatalytic activity was measured using RB5 and RO16 to explain the influence of the incorporation of SiO<sub>2</sub> and GO in TiO<sub>2</sub> nanofibers. The study utilized visible-light irradiation for the decolorization of the reactive black 5 and compared photocatalytic activity

for three cases: without any SiO<sub>2</sub> or GO nanoparticles, with 2% % by weight of SiO<sub>2</sub>, and 6% by weight of SiO<sub>2</sub> with a fixed amount of graphene oxide incorporated in TiO<sub>2</sub> nanofibers. Literature showed that the higher photocatalytic performance is highly linked to a larger area of the surface [21], while the lower photo activity is probably ascribed to the photoexcited electron and positive hole recombination at defects[22]. As Figure 6 displays, the synthesized photocatalyst of SiO<sub>2</sub>&GO/ TiO<sub>2</sub> significantly improved the degradation rate of the dye.

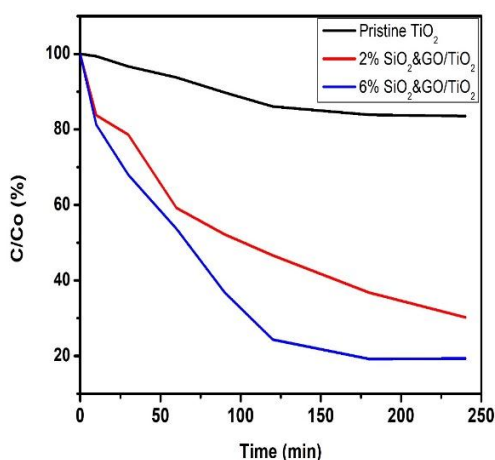


Figure 6: Photocatalytic degradation of RB 5 by TiO<sub>2</sub>, and by different compositions of SiO<sub>2</sub>&GO incorporated TiO<sub>2</sub>.

Comparing the SiO<sub>2</sub>&GO/ TiO<sub>2</sub> results with the TiO<sub>2</sub> nanofiber confirms enhanced degradation of the reactive black 5 in this experiment. The better photocatalytic activity of the SiO<sub>2</sub>&GO/TiO<sub>2</sub> photocatalyst than other photocatalysts resulted primarily from the effect of coupling of TiO<sub>2</sub>, SiO<sub>2</sub>, and GO after 160-min of irradiation. The catalyst Nfs (6% SiO<sub>2</sub> wt) showed RB 5 removal efficiency of 86 %, which is much higher than 60 % over SiO<sub>2</sub>&GO/TiO<sub>2</sub> (2% GO wt), and 19% over bare TiO<sub>2</sub> NFs. Furthermore, SiO<sub>2</sub>&GO/TiO<sub>2</sub> NFs (6 % GO wt) exhibited better performance of photocatalytic activity than the other photocatalysts, which benefited from the GO adsorptive capacity and separation of high charge and the high affinity of nano silica toward the dye molecules. The obtained efficiency is comparable to 54% dye removal when using GO [23], 63.8% removal by using macadamia seed Husks [24], 77.2% removal using peanut hull [25], 75% removal by N-doped TiO<sub>2</sub> DLHF[26], and 78.91% removal when using Hexadecylamine Impregnated Chitosan-Powdered Activated Carbon Beads [27] Which made our results satisfying with other removal efficiency. The improvement is attributed to efficient transmission of

the charge between TiO<sub>2</sub> and SiO<sub>2</sub>, which increases the charge carriers' lifetime. furthermore, the particle size and the surface contact between particles govern the catalyst's photocatalytic activity. The proper amount of SiO<sub>2</sub>, SiO<sub>2</sub> nanoparticles incorporated in TiO<sub>2</sub> reduces the recombination between the electrons and the holes, improving the efficiency of the photocatalytic activity of TiO<sub>2</sub> [28].

First, photocatalysis moves pollutants from the solution to the catalyst surface. Therefore, the adsorption capacity is a crucial indicator of the degradation ability of the catalyst. As the adsorption of pollutants increases, the reaction of photodegradation accelerates. The adsorption experiment of the dye solution was performed in the dark for 4 h on the photocatalyst containing 6% SiO<sub>2</sub> NPs. As figure 7 explains, the TiO<sub>2</sub> catalyst removed about 19 % of the RB 5, compared to 86% dye removal by photodegradation in the presence of SiO<sub>2</sub>&GO/TiO<sub>2</sub> nanofibers. The results implied that nano silica and GO positively influenced the photodegradation of the reactive black 5. SiO<sub>2</sub> nanoparticles play, first, the role of an additional adsorbent adsorbing the dye, which subsequently diffuses to the catalyst surface to effectively decompose. As a result, the remaining dye molecules in the solution are adsorbed onto the empty locations.

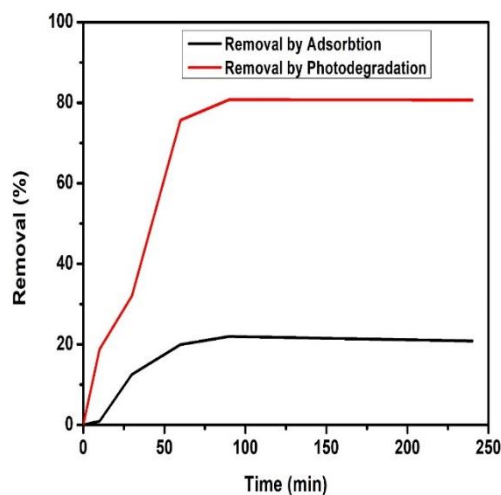


Figure 7: Removal efficiency due to Adsorption and photodegradation of RB 5% in presence of SiO<sub>2</sub>/GO incorporated TiO<sub>2</sub> NFs.

Furthermore, at the proper GO amount, GO nanoparticles incorporated in TiO<sub>2</sub> hinder the recombination between the electrons and the holes, improving the efficiency of the photocatalytic activity of TiO<sub>2</sub>. As the content of the GO increases, the density of oxygen-containing functional groups, such

as hydroxyl groups, increases, enhancing the ionic/electro interaction and, therefore, better absorptivity. Furthermore, GO acts as an electron acceptor, accelerating the process of interfacial electron-transfer from TiO<sub>2</sub>, obstructing the charge carriers' recombination, and enhancing the photocatalysis process[29]. Moreover, the photosensitizing properties that GO may possess and the composites of TiO<sub>2</sub>/graphene oxide increase the absorption of light into the visible region. Consequently, TiO<sub>2</sub>/GO nanofibers show the coupling effect of adsorption and photocatalysis, significantly increasing the efficiency of dye degradation.

### 3.3. Kinetic study of the degradation of RB5

For most of the organic pollutants, such as RB5, the photocatalytic degradation kinetics under visible-light irradiation is modeled using Langmuir–Hinshelwood (L-H) model, which is a first-order reaction where the rate of degradation constant is estimated as the equation shows [30, 31]:

$$-\ln\left(\frac{C}{C_0}\right) = kt$$

While C<sub>0</sub> is the initial dye solution's concentration, C is the concentration of the dye solution after photocatalytic reaction at time t, and k (min<sup>-1</sup>) is the constant of the reaction rate. The line slope of the graphing -ln(C/C<sub>0</sub>) against the time of irradiation for each synthesized photocatalyst can be used to estimate the k constant. Figure 8 illustrates the best fit between the data from the experimental work and the behavior of the L-H model for SiO<sub>2</sub>&GO/TiO<sub>2</sub> nanophotocatalyst. As the figure displays, the k constant of the best nanophotocatalyst was estimated at 0.004 min<sup>-1</sup> with an R<sup>2</sup> value of 0.979.

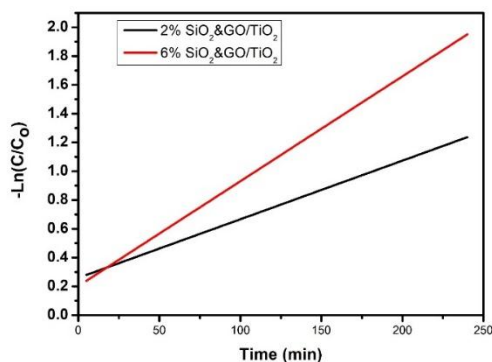


Figure 8: Data modeling according to Langmuir-Hinshelwood model the photocatalysts.

### 3.4. Repetitive use of SiO<sub>2</sub>&GO/TiO<sub>2</sub> NFs

The study employed the same photocatalyst to successively perform three cyclic tests. A 20 mg-sample was successively utilized to degrade 50 mL of the dye solution (10ppm). As figure 9 illustrates, for the first and second cycles, the efficacy of the initial photocatalyst used is almost similar to that of the reused photocatalyst for the degradation of RB5. However, in the third cycle, the efficacy significantly declines, possibly due to the decline in the number of active locations.

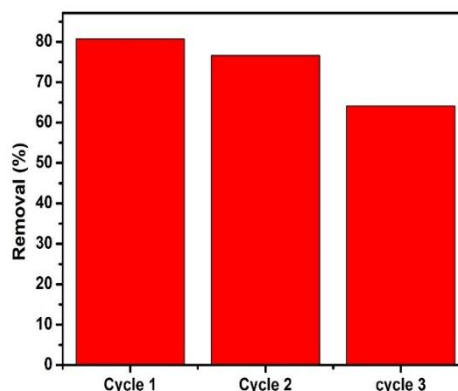


Figure 9: Efficiency of SiO<sub>2</sub>/GO/ TiO<sub>2</sub> for several usages for RB 5 removal.

Additionally, the photocatalytic activity of the SiO<sub>2</sub>&GO /TiO<sub>2</sub> composites was tested by the RO16 degradation. As Figure 10 shows, the photocatalytic performance of the catalyst was very satisfactory, when the process was performed under visible light, about 55% of the dye was degraded.

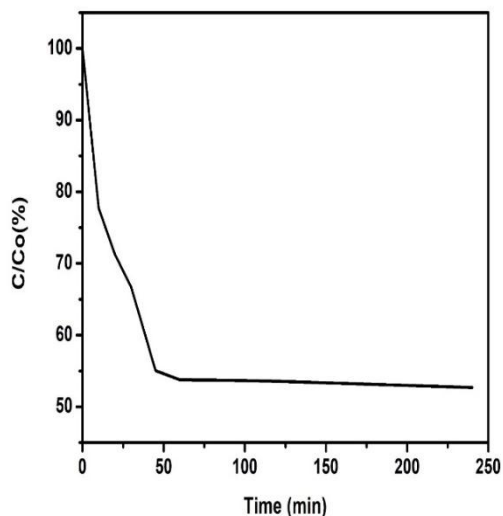


Figure 10: Rate of degradation of reactive orange 16 on SiO<sub>2</sub>&GO/TiO<sub>2</sub> photocatalyst

#### 4. Conclusion

Azo dyes, such as Reactive Black 5 (RB5), are commercially the most produced dyes annually and widely used in the textile industry due to their stabilities and simple dyeing procedures. However, about 50% of the total amount of RB5 used is lost and dumped in the surrounding environment. Silicon dioxide and graphene oxide nanoparticles, incorporated with titanium dioxide nanofibers, were developed for a photocatalytic process. To produce the nanofiber mats, the current study employed an electrospinning technology and used a polymeric solution containing nano silica and nano graphene oxide. The synthesized nanofibers were calcined at 680 °C in air. Then, the synthesized catalyst was characterized and utilized to degrade the RB5 and RO16. As the results revealed, the SiO<sub>2</sub> and GO NPs addition to the pristine TiO<sub>2</sub> enhanced the dye removal, demonstrating a higher photocatalytic activity than using pure TiO<sub>2</sub>. The improvement is maybe due to the high retard in electron recombination and increased adsorptive activity. Moreover, the results suggested that the synergy effect of silica and graphene oxide adsorption and TiO<sub>2</sub> photocatalysis efficiently degraded the dye. Good recyclability of the synthesized photocatalyst was observed, demonstrating the high stability of the obtained nanofibers. The obtained results explore new prospects for photocatalysts' design and fabrication.

#### References

[1] A. Fujishima and K. Honda, "Electrochemical photolysis of water at a

- semiconductor electrode," *nature*, vol. 238, pp. 37-38, 1972.
- [2] B. Bakbolat, C. Daulbayev, F. Sultanov, R. Beissenov, A. Umirzakov, A. Mereke, *et al.*, "Recent developments of TiO<sub>2</sub>-based photocatalysis in the hydrogen evolution and photodegradation: a review," *Nanomaterials*, vol. 10, p. 1790, 2020.
- [3] H. M. Mousa, J. F. Alenezi, I. M. Mohamed, A. S. Yasin, A.-F. M. Hashem, and A. Abdal-hay, "Synthesis of TiO<sub>2</sub>@ZnO heterojunction for dye photodegradation and wastewater treatment," *Journal of Alloys and Compounds*, vol. 886, p. 161169, 2021.
- [4] J. Singh, S. Kumar, A. K. Manna, and R. Soni, "Fabrication of ZnO–TiO<sub>2</sub> nanohybrids for rapid sunlight driven photodegradation of textile dyes and antibiotic residue molecules," *Optical Materials*, vol. 107, p. 110138, 2020.
- [5] S. V. Kite, A. N. Kadam, D. J. Sathe, S. Patil, S. S. Mali, C. K. Hong, *et al.*, "Nanostructured TiO<sub>2</sub> sensitized with MoS<sub>2</sub> nanoflowers for enhanced photodegradation efficiency toward methyl orange," *ACS omega*, vol. 6, pp. 17071-17085, 2021.
- [6] R. A. Aziz and I. Sopyan, "Synthesis of TiO<sub>2</sub>-SiO<sub>2</sub> powder and thin film photocatalysts by sol-gel method," 2009.
- [7] G. M. Tolba, N. A. Barakat, A. Bastaweesy, E. Ashour, W. Abdelmoez, M. H. El-Newehy, *et al.*, "Effective and highly recyclable nanosilica produced from the rice husk for effective removal of organic dyes," *Journal of Industrial and Engineering Chemistry*, vol. 29, pp. 134-145, 2015.
- [8] G. M. Tolba, A. Bastaweesy, E. Ashour, W. Abdelmoez, K. A. Khalil, and N. A. Barakat, "Effective and highly recyclable ceramic membrane based on amorphous nanosilica for dye removal from the aqueous solutions," *Arabian Journal of Chemistry*, vol. 9, pp. 287-296, 2016.
- [9] J.-F. Guo, B. Ma, A. Yin, K. Fan, and W.-L. Dai, "Photodegradation of rhodamine B

- and 4-chlorophenol using plasmonic photocatalyst of Ag–AgI/Fe<sub>3</sub>O<sub>4</sub>@ SiO<sub>2</sub> magnetic nanoparticle under visible light irradiation," *Applied Catalysis B: Environmental*, vol. 101, pp. 580-586, 2011.
- [10] N. d. C. L. Beluci, G. A. P. Mateus, C. S. Miyashiro, N. C. Homem, R. G. Gomes, M. R. Fagundes-Klen, *et al.*, "Hybrid treatment of coagulation/flocculation process followed by ultrafiltration in TiO<sub>2</sub>-modified membranes to improve the removal of reactive black 5 dye," *Science of The Total Environment*, vol. 664, pp. 222-229, 2019.
- [11] M. Alaguprathana, M. Poonkothai, F. Ameen, S. A. Bhat, R. Mythili, and C. Sudhakar, "Sodium hydroxide pre-treated *Aspergillus flavus* biomass for the removal of reactive black 5 and its toxicity evaluation," *Environmental Research*, vol. 214, p. 113859, 2022.
- [12] M. N. Chong, Y. J. Cho, P. E. Poh, and B. Jin, "Evaluation of Titanium dioxide photocatalytic technology for the treatment of reactive Black 5 dye in synthetic and real greywater effluents," *Journal of Cleaner Production*, vol. 89, pp. 196-202, 2015.
- [13] F. H. de Oliveira Alves, O. A. Araújo, A. C. de Oliveira, and V. K. Garg, "Preparation and characterization of PANi (CA)/Magnetic iron oxide hybrids and evaluation in adsorption/photodegradation of blue methylene dye," *Surfaces and Interfaces*, vol. 23, p. 100954, 2021.
- [14] Y. Lu, Y. Cai, S. Zhang, L. Zhuang, B. Hu, S. Wang, *et al.*, "Application of biochar-based photocatalysts for adsorption-(photo) degradation/reduction of environmental contaminants: mechanism, challenges and perspective," *Biochar*, vol. 4, pp. 1-24, 2022.
- [15] M. Obaid, G. M. Tolba, M. Motlak, O. A. Fadali, K. A. Khalil, A. A. Almajid, *et al.*, "Effective polysulfone-amorphous SiO<sub>2</sub> NPs electrospun nanofiber membrane for high flux oil/water separation," *Chemical Engineering Journal*, vol. 279, pp. 631-638, 2015.
- [16] Y. Wang, X. Liu, L. Guo, L. Shang, S. Ge, G. Song, *et al.*, "Metal organic framework-derived C-doped ZnO/TiO<sub>2</sub> nanocomposite catalysts for enhanced photodegradation of Rhodamine B," *Journal of Colloid and Interface Science*, vol. 599, pp. 566-576, 2021.
- [17] M. Bellardita, M. Addamo, A. Di Paola, G. Marci, L. Palmisano, L. Cassar, *et al.*, "Photocatalytic activity of TiO<sub>2</sub>/SiO<sub>2</sub> systems," *Journal of Hazardous Materials*, vol. 174, pp. 707-713, 2010.
- [18] M. Jesus, A. Ferreira, L. Lima, G. Batista, R. Mambrini, and N. Mohallem, "Micro-mesoporous TiO<sub>2</sub>/SiO<sub>2</sub> nanocomposites: Sol-gel synthesis, characterization, and enhanced photodegradation of quinoline," *Ceramics International*, vol. 47, pp. 23844-23850, 2021.
- [19] D. Ramos, M. V. González, R. Muñoz, J. S. Cruz, D. Moure-Flores, and S. Mayén-Hernández, "Obtaining and characterization of TiO<sub>2</sub>-GO composites for photocatalytic applications," *International Journal of Photoenergy*, vol. 2020, 2020.
- [20] Y. Zhao, C. Li, X. Liu, F. Gu, H. Du, and L. Shi, "Zn-doped TiO<sub>2</sub> nanoparticles with high photocatalytic activity synthesized by hydrogen–oxygen diffusion flame," *Applied Catalysis B: Environmental*, vol. 79, pp. 208-215, 2008.
- [21] H. D. Jang, S.-K. Kim, and S.-J. Kim, "Effect of particle size and phase composition of titanium dioxide nanoparticles on the photocatalytic properties," *Journal of Nanoparticle Research*, vol. 3, pp. 141-147, 2001.
- [22] M. V. Dozzi, A. Candeo, G. Marra, C. D'Andrea, G. Valentini, and E. Selli, "Effects of photodeposited gold vs platinum nanoparticles on N, F-doped TiO<sub>2</sub> photoactivity: a time-resolved photoluminescence investigation," *The*

- Journal of Physical Chemistry C*, vol. 122, pp. 14326-14335, 2018.
- [23] N. A. Travlou, G. Z. Kyzas, N. K. Lazaridis, and E. A. Deliyanni, "Graphite oxide/chitosan composite for reactive dye removal," *Chemical engineering journal*, vol. 217, pp. 256-265, 2013.
- [24] M. M. Felista, W. C. Wanyonyi, and G. Ongera, "Adsorption of anionic dye (Reactive Black 5) using macadamia seed husks: kinetics and equilibrium studies," *Scientific African*, vol. 7, p. e00283, 2020.
- [25] M. Ş. Tanyildizi, "Modeling of adsorption isotherms and kinetics of reactive dye from aqueous solution by peanut hull," *Chemical Engineering Journal*, vol. 168, pp. 1234-1240, 2011.
- [26] R. Kamaludin, A. S. M. Puad, M. H. D. Othman, S. H. S. A. Kadir, and Z. Harun, "Incorporation of N-doped TiO<sub>2</sub> into dual layer hollow fiber (DLHF) membrane for visible light-driven photocatalytic removal of reactive black 5," *Polymer Testing*, vol. 78, p. 105939, 2019.
- [27] M. Vakili, H. M. Zwain, A. Mojiri, W. Wang, F. Gholami, Z. Gholami, *et al.*, "Effective adsorption of reactive black 5 onto hybrid hexadecylamine impregnated chitosan-powdered activated carbon beads," *Water*, vol. 12, p. 2242, 2020.
- [28] N. Esfandiari, M. Kashefi, M. Mirjalili, and S. Afsharnezhad, "On the adsorption kinetics and mechanism of enhanced photocatalytic activity of Fe<sub>3</sub>O<sub>4</sub>-SiO<sub>2</sub>-TiO<sub>2</sub> core-multishell nanoparticles against E. coli," *Journal of Biomedical Materials Research Part A*, vol. 109, pp. 181-192, 2021.
- [29] I. V. Lightcap, T. H. Kosel, and P. V. Kamat, "Anchoring semiconductor and metal nanoparticles on a two-dimensional catalyst mat. storing and shuttling electrons with reduced graphene oxide," *Nano letters*, vol. 10, pp. 577-583, 2010.
- [30] F. Temerov, B. Ankudze, and J. J. Saarinen, "TiO<sub>2</sub> inverse opal structures with facile decoration of precious metal nanoparticles for enhanced photocatalytic activity," *Materials Chemistry and Physics*, vol. 242, p. 122471, 2020.
- [31] G. Sodeifian and R. Behnood, "Hydrothermal synthesis of N-doped GQD/CuO and N-doped GQD/ZnO nanophotocatalysts for MB dye removal under visible light irradiation: evaluation of a new procedure to produce N-doped GQD/ZnO," *Journal of Inorganic and Organometallic Polymers and Materials*, vol. 30, pp. 1266-1280, 2020.